



Moon body resonance

M Omerbashich

► To cite this version:

M Omerbashich. Moon body resonance. Journal of Geophysics, 2019,
<https://n2t.net/ark:/88439/x034508>, 63 (1), pp.30-42. hal-02270359

HAL Id: hal-02270359

<https://hal.science/hal-02270359>

Submitted on 24 Aug 2019

HAL is a multi-disciplinary open access archive for the deposit and dissemination of scientific research documents, whether they are published or not. The documents may come from teaching and research institutions in France or abroad, or from public or private research centers.

L'archive ouverte pluridisciplinaire **HAL**, est destinée au dépôt et à la diffusion de documents scientifiques de niveau recherche, publiés ou non, émanant des établissements d'enseignement et de recherche français ou étrangers, des laboratoires publics ou privés.



Distributed under a Creative Commons Attribution - NonCommercial - NoDerivatives 4.0 International License

Moon Body Resonance

Mensur Omerbashich

PO Box 1, Sarajevo Bosnia | hm@royalfamily.ba

The full range of 50 initial, Moon-orbit-forced superharmonic resonance periods is detected in the 1969–1977 time-series of all 12474 consecutive 0.02 Hz moonquakes from the Apollo Program catalog. The resonance is found forcing the strongest-energy (highest-fidelity) part of the 10 hours–100 days (27.78–0.115741 μHz) long-periodic band at 99–67% confidence as well as below. Resonance signatures of the Moon's other four long tidal periods – synodic, anomalistic, nodical, and tropical – were also identified but not as separate drivers of body resonance. The spectra were computed using a least-squares spectral analysis method that enabled separation of the signal driver and noise signatures of all lunar tides, as well as extraction of the exact sequence of resonant subperiods affecting the solid Moon. Thus lunar seismotectonics is forced by the Moon's orbital period as the disruptive phase that introduces nonlinearity into lunar vibration, giving rise to superharmonic resonance and probably the so-called free librations as well. The earlier computation of the Earth superharmonic resonance and this computation of the Moon superharmonic resonance constitute conclusive proof of the universality of body mechanical resonance in astronomical bodies, as well as of the driving role of geophysics as a catalyst of life.

resonance computations; Moon tectonics; moonquakes; moonquake prediction; planetary physics

1. Introduction

Following the demonstration of Earth body resonance from time-series of Mw5.6+ earthquakes spanning 3.3178 years (Omerbashich, 2019a), I proceed to identify the resonant tidal response of the Moon as a nonlinear system. Basically, an attempt is made here to detect the forcing period $T \in \mathbb{R}$ that causes the Moon's own linear (tidal) response as well as any additional nonlinear vibration $n / (mT) \in \mathbb{N}$ – termed *subharmonic* for $n / m \in (0, 1)$: $n > 1 \wedge n \in \mathbb{N}$ or *superharmonic* for $n / m > 1 \wedge n / m \in \mathbb{R}$ (Yang et al., 2016). The basic methodology of identifying body resonance and parameters from spectra of seismicity time-series are in (Omerbashich, 2019a).

The phenomenon of *resonating vibration* or just *resonance* occurs when a physical system's natural period of oscillation coincides with another physical system's period of oscillation (or its fractional multiple). We speak of *electrical resonance* when the system consists of one or more electrical circuits, or *mechanical resonance* when the system consists of one or more bodies of mass. Specifically, matching one system's natural period with another system's subharmonic vibration period or its fractional multiple gives rise to *subharmonic resonance*. Similarly, matching of one system's natural period of vibration with another system's superharmonic vibration period or its fractional multiple gives rise to *superharmonic resonance*. Thus in solids, structural failure occurs along a resonance period via frequency-demultiplication as one of the rarest mechanical phenomena in Nature, known for its ability to magnify the energy injected at the fundamental disturbing frequency by 100s of times. (Den Hartog, 1985)

Subharmonic and superharmonic resonances can develop in discrete regions of a physical system. As with all solids, the hundreds of tectonic plates and brittle regions in the upper mantle constitute Earth's vibrating parts, while those in the Moon remain elusive. Based on research finds from mechanical and electrical engineering, subharmonic resonances typically occur at periods shorter than (usually fractions of) the long-periodic excitation; superharmonic resonances, at the periods longer than (usually integer multiples of) the long-periodic excitation. Most nonlinear systems exhibit simplistic super-harmonic resonant periods n / T as a special case $m = 1$. Importantly, resonating linear-systems are a special case of subharmonic resonators (Yang et al., 2016), which is a critical constraint for this demonstration.

Since previous spectral analyses of moonquakes occurrences – performed under the assumptions of Moon system's linearity or simple nonlinearity – found no periodicity other than a few tidal signals, here of interest is a strictly nonlinear (subharmonic and superharmonic) signal $T_{R\text{sup}}$, as the only unexplored path. This necessitates looking into the long-periodic band commonly referred to as “long-periodic noise” which starts here at the as-of-yet-unknown or largely uncertain Moon's natural period of vibration, encompasses the orbital period as the likely forcer phase, then the astronomical periods, and ends at the lunar-synodic month period. Much like lunar forcing was considered part of the signal to demonstrate the Earth body resonance, here Earth's *geoforcing* of the Moon is a crucial part of the signal and not noise as in classical approaches.

So in the following, I consider the Moon under nonlinear forcing as prescribed by the georesonator hypothesis, which I herewith tacitly assume applies to all macroscopic bodies of mass. Note again that, for resonant (nonlinear) components of vibration to occur, it does not matter where this nonlinearity originates – in the source mechanism, in the damping, or both (Den Hartog, 1985). Finally, to model the Moon as a fully nonlinear forced system in which one could expect anything, it is prudent to recall once again that a single external excitation always induces superharmonic resonances only (Yang et al., 2016).

2. Signal

In search of a complete sequence of Moon body resonance subperiods (the signal), I consider all 13,058 seismic events in the 1981 (updated in 2008) *Levent.1008* Moonquakes Catalog of the Apollo Program's passive seismic experiment ALSEA, spanning 1969-1977 Missions 11, 12, 14, 15, and 16, and sampled at the 0.02 Hz, or once-per-minute, rate (Nakamura et al., 1981); hereafter: the Moon Catalog. Catalog times were in Earth days, Earth hours, and Earth minutes (henceforth: days, hours, and minutes, respectively). The specific coverage was: 71 events from 1969, 624 from 1970, 1,912 from 1971, 3,007 from 1972, 1,896 from 1973, 1,376 from 1974, 1,087 from 1975, 1,612 from 1976, and 1,473 from 1977. Here the minor correction of 2018, *Levent.1008c*, was not used because the documentation did not specify corrections and because it labeled them apriori as overall insignificant.

After the removal of 15 erroneously time-stamped events and 569 time-duplicates (i.e., doublet, triplet, and quadruplet events with the same time-stamp, preventing time-series monotony), the remaining 12,474 seismic events were spectrally analyzed. This removal of 4% data was acceptable because, as shown for the Earth body resonance, the removal of 2% of earthquakes from a much denser dataset did not affect that demonstration based on 15 times fewer events spanning less than half the interval of moonquakes used in here (Omerbashich, 2019a). Note that the selenophysics community relies extensively on the here used seismic observations from the ALSEA experiment; an extensive review of those activities and studies can be found in, e.g., (Khan et al., 2013). Of relevance here is that past spectral analyses of deep moonquakes occurrences have claimed Moon's linear periodic response, of ~13 days, 27 days, and 206 periodicities; see, e.g., (Bulow et al., 2007).

3. Data analysis

The spectra were computed using the Gauss-Vaníček spectral analysis (GVSA) method (Vaníček, 1969) (Vaníček, 1971), as $s_j^{GVSA}(T_j, M_j^{GVSA})$; $j = 1 \dots k \wedge k \in \aleph$, with $k = 1000 \wedge k = 2000$ spectral resolutions. The GVSA falls in the Least Squares Spectral Analysis class of spectral methods which fit data with trigonometric functions. The GVSA is preferred over the Fourier class of spectral analysis methods (FSA) for analyzing raw records of unevenly spaced real data (Press et al., 2007). As variance-based, GVSA provides a straightforward statistical analysis with a linear depiction of background noise levels (Omerbashich, 2004; 2006). GVSA is one of the most accurate methods of numerical analysis (Omerbashich, 2019b), enabling absolute accuracy, i.e., accuracy in extracting a period from big and raw data sets with 10s of billions of measurements, of down to twice the sampling rate (Omerbashich, 2004; 2007; 2019a; 2019b).

The record contained over 7,000 tidal (deep and shallow) moonquakes as the dominant type. Here data were not manipulated unlike in the Fourier class of spectral analysis methods. Instead, spectral computations benefited the most from the GVSA's inherent ability to analyze raw data, as variance spectra thrive on the background or ambient noise. Sporadic seismic events, including around 1,700 meteorite impacts on the Moon's surface and about ten Lunar Module's touchdowns and booster firings, were left in the record since they all leave inharmonic signatures. Likewise, some 3,500 thermal-expansion events – driven by the change of day and night – were kept too; but since they leave harmonic imprints, those events were kept to boost the spectral magnitudes by consolidating (overall-tuning) the noise. Namely, given the Moon's said tidal lock with that same phase, equaling one Moon day, this day-night periodicity coincides with the signal driver and enhances it further. At the same time, polluting the signal by the thermal-expansion events to the point of a biased result is not an issue here, since those events are mostly shallow and thus do not critically affect the whole-body resonance – specifically, the most energetic band that controls most of the mass and drives the body. Analogously to the Earth body resonance case, the “driver” here marks that (external) forcing phase which dominated the longest-periodic part of the Moon natural band. Likewise, the demonstration from seismicity occurrence (times) means direct detection of resonance as earthquakes occur (“ride on it”), not as they leave imprints onto some intermediary proxy - in which case secondary phenomena like thermal expansion could matter and would need to be accounted for as obviously affecting the analyses (here analyses include no proxies). Even if the Moon had an atmosphere, thermal variations (in fact: air molecules oscillations and corresponding gas resonances), do not carry sufficient power to excite the matter in its longest (of solids) band of vibration. Note also that the concept of adding noise to enhance the signal-to-noise ratio, known as stochastic resonance, has been demonstrated in many fields including the application of the GVSA in geophysics; see (Omerbashich, 2008). Finally, leaving meteorite impact events in moonquake records for signal enhancement is a standard procedure, e.g., in processing source waveforms.

Unlike the 1 Hz quality catalogs used in the demonstration of Earth body resonance, the Moon catalogs still lack a seismic magnitudes system uniquely related to source energy emissions. Thus, despite some attempts to define magnitudes, there is no consistent definition of moonquake magnitude (Nakamura, 2019). This regrettable circumstance half a century since the Apollo program confines one to spectral analyses of noisy time-series and prevents estimating the physically most likely cutoff-magnitude for defining the overall energy levels of Moon resonance tectonics.

So to mimic earthquake records for the Moon, I arbitrarily assign to each event in the Moonquake Catalog a generic (random) seismic magnitude in undeclared units, from the [5.5, 7.5] interval. Although such magnitude range is physically unrealistic for the Moon as moonquakes are mostly in the Mw2-5 range, such a scale-up to mimic the case of the earthquakes is justified statistically since it helps spectral resolution to follow the boost in spectral magnitudes (from noise additions via keeping the

meteorite-impact and thermal-expansion events in the raw record). Most importantly, such an approach does not affect the signal itself because in the whole-body forcing the (longest-periodic segment of the) signal is overwhelmingly stronger than any noise signature or all the signatures combined (Omerbashich, 2019a). In principle, strong noise imprints by Moon's various candidate-forcers are comparable as well as pure (complete) signals are. Any other use of differentials in applied science works in the same way; say, the DGPS. This *differential spectral analysis* then makes the core of this paper. A convenient circumstance here is that all of the compared signals entertain mostly systematic noise and feature mutually like statistics.

Mimicking of earthquake records has been used in compiling moonquake source spectra as well so that moonquakes' standard compressed plots are generic. Thus the signal envelope amplitudes for moonquakes are in millimetres on a standard plot as created by taking the absolute value of the difference between consecutive long-periodic data points, summing, and plotting them at a scale but in alternating polarities to give the appearance of a seismogram (Nakamura et al., 1981).

As seen from the demonstration of Earth body resonance, time-series of major catalogs of earthquakes possess a high degree of internal consistency, robustness, and ambiguity – as expected from data which describe a constantly but inconsistently driven physical process. As it turned out, those data indeed described a genuine albeit nonlinear behavior of a physical system. (Omerbashich, 2019a) However, no such information can be expected from the moonquake data as they are generally of lower quality, i.e., overburdened with ambient and unknown noise, collected with unmaintained instruments, missing uniquely defined seismic magnitudes, etc. Nonetheless, the moonquake data are uniquely ambiguous when taken as a whole, which suffices for spectral analyses in this differential demonstration of the whole-body resonance of the Moon.

Also looked into were the short-periodic spectral bands: 2'-15 days and 2'-100 days, which all returned active pure noise indicative of long-periodic excitation. Other inspected long-periodic bands included: 5h-30 days, 5h-60 days, 5h-100 days, 400'-100 days, 5h-150 days, and 5h-180, but results from those bands were found not as useful as the results from the primary band of interest, of 10 h–10 days.

The demonstration here differs from that of the Earth case fundamentally as well because unlike the Earth's natural mode, the Moon's natural period of oscillation is unknown or difficult to estimate at best. Estimates of the Moon mantle's viscosity vary greatly, and there are no reliable reference models of the Moon (Khan et al., 2013). Fortunately, thanks mainly to the Earth-Moon tidal lock the Moon's orbital period (time to complete one orbit with respect to stars; also called sidereal period), of $T_M = 27.32166$ days, is the only real candidate for the Moon's external forcing phase as well. Namely, the T_M introduces nonlinearity into the Moon's tidal response supposedly constantly while the already synchronized Moon keeps trying to resynchronize spatially with the ever-escaping Earth at precisely T_M . While this simple state of affairs indeed is a fortunate circumstance, it makes the demonstration here more laborious than for the Earth, because the Moon experiences several long-periodic tides so close to the orbital period that their potential for creating own long-periodic body resonance(s) must also be analyzed.

Thus another tidal period that could be reflected in (mixed with) the *pure signal* is the Moon's synodic month (time between two same lunar phases), of $T_S = 29.53059$ days. (By pure signal, I mean the moonquakes on a mathematically idealistic, uncoupled, and undisturbed body of mass so that all other Moon vibration is considered noise - unlike the classical view in which moonquakes are regarded to be the seismic signal.) In addition, there are relevant astronomical lunar periods that include: one anomalistic month (average time the Moon takes between two perigees; offset from the orbital period due to Moon's apsidal precession, of 8.8 years), of $T_A = 27.55455$ days, one nodical month (average time the Moon takes to return to the same node; offset from the orbital period due to Moon's nodal precession, of 18.6 years), of $T_N = 27.21222$ days, and one tropical month (average time of the Moon's crossing of the same equinox twice consecutively; slightly offset from the orbital period due to Earth's axial precession ("of equinoxes"), of about 26,000 years), of $T_T = 27.32158$ days (Seidelmann, 1992). However, all these arbitrarily defined periods (with values averaged over the varying Moon's trajectory as due to vari-

ous precessions) are of a considerable vertical pull – of up to a few dm – which normally thwarts any secondary vibration so they cannot be expected to give rise to a (primarily horizontally-moving) long-periodic body resonance.

As surmised earlier, a variation in seismic magnitudes enables validation of a preset cutoff magnitude and the corresponding physical process behind spectrally analyzed seismicity occurrence (Omerbashich, 2019a). An additional benefit of comparing the spectra of noisy moonquake v. impeccable M_w 5.6+ earthquake occurrences lies in revealing the physics of the extreme-energies band of the Moon. If such two dissimilar (presumably independent) datasets produce similar variance-spectra, then the working assumption here is that not only do those datasets describe a common astrophysical mechanism but such mechanism could only arise due to the Earth-Moon tidal system. As mentioned in the above, missing unique moonquake magnitudes were simulated here. So if the Moon and the Earth variance spectra show resemblance, nature (and therefore type too) of seismic magnitudes will be irrelevant for establishing the existence and type of body resonance via differential spectral analysis that looks into different lunar candidate-forcers. It would then be justifiable to use randomly generated seismic magnitudes. Based on what is known now on the Earth body resonance and the variance-spectral response to that resonance, this reverse-engineering process is also helpful for determining the Moon's natural period of oscillation from real data. Unfortunately, as already mentioned, a reliable whole-body selenophysical reference model from inversions is still missing due to sectored seismic coverage of the Moon and for other reasons.

While all bodies tend to synchronize (Pikovsky et. al., 2001), the Moon has already attained its synchronization with the Earth, both spatially in the form of tidal (orbital-rotational) lock and temporally in the form of coupling of the natural periods of vibration at both macroscopic and quantum scales (Omerbashich, 2007). That is a fortunate circumstance for this demonstration, one that takes away a degree of freedom from the Earth-Moon coupled oscillator. Thus Moon body resonance, if its signature is present in moonquakes occurrences records, occurs under nonlinear forcing due to the Moon orbital period's continuous attempts at resynchronization of the already synchronized Moon and Earth. Here it is important to recall that such a situation usually results in a superharmonic resonance (Yang et. al. 2016).

Although Moon seismicity lacks global coverage, a sectored coverage of the ALSEA experiment (that nonetheless snapped nearly half the Moon) suffices here because the seven-year data span from the relatively non-rotating Moon is enough to establish or rule-out any nonlinear periodicities. Note again that the cyclic events due to the day-and-night thermal variation as a primary component of the Moon's ambient noise do not dominate the record. Furthermore, the absence of an atmosphere and so of atmospheric tides or gusty winds to account for in spectral analyses is of no particular benefit here because those tides would be a useful part of the signal. Namely, as with the demonstration of Earth body resonance, here too we deal with extreme energy bands to which those tides if existed, would be a minor contributor. As with exploring the Earth body resonance, here as well I tacitly assume that all spectral estimates at different confidence levels are physically meaningful if at least 67% reliable. The success of the methodology applied in (Omerbashich, 2019a) justifies such an approach.

As outlined in the above, that success can be applied oppositely as well, in a *bona fide* twist: since the data are of an undeclared but likely low quality, I regarded that vital shortcoming as an attribute which I then pushed to the fullest extent – by actually contaminating the data with the record's complete information and then looking not just for the parts of the signal above but also those below the 67% significance level. While not justified from the strictly statistical point of view, this is justified from the physics point of view because the physical process of resonance seismotectonics has already been demonstrated for the Earth and found to be statistically significant. Then detecting even such a process's noise signature (of course alongside at least partial detection above a significance level) on another astronomical body in that body's long-periodic band would strongly indicate if not verify the presence of the same phenomenon on that other body as well. Conversely, the detection of resonance seismotectonics in the noisy record of moonquakes occurrences would add both extraterrestrial

(methodological) and statistical (robustness) credibility to the demonstration of the Earth's resonance seismotectonics demonstrated earlier from impeccable datasets. In other words, the proof of planetary resonance seismotectonics would then be complete. Undoubtedly, the Fourier class of spectral analysis methods is useless in the above approach to treating noisy natural datasets that cannot be usefully denoised.

Indeed, the preliminary spectrum on Figure 1 shows that, as variance percentage levels went down in absolute terms more than an order of magnitude relative to Figure 2 in (Omerbashich, 2019a), the resemblance of the Earth spectra is remarkable. At the same time, the significance of each of the preliminary spectral magnitudes has indicated that there is only one superharmonic resonance of the solid Moon, Figure 2. And since a solitary superharmonic resonance always implies a single external forcing (Yang et. al. 2016), further investigations to identify the period that forces the Moon resonance and seismotectonics are justified.

Recall that statistical fidelity $\Phi > 12$ in physical data indicates a physically meaningful result (Omerbashich, 2006). Since classical (ambient) noise here mainly became part of the signal - causing spectral magnitudes to drop an order of magnitude or more from the Earth body resonance demonstration - the fidelities that define the strongest-energies subband (here the ten $\Phi \geq 1$ lead periods of a resonance train) also dropped a magnitude of order. Thus a signal with $\Phi \in (\sim 1, \sim 12)$ can now be considered physically significant for the Earth-Moon physical system. By the same standard then (considering the Earth and the Moon as a single oscillator), the infinitesimal fidelities $0 \leq \Phi < 1$ shall define the signal's imprint in noise.

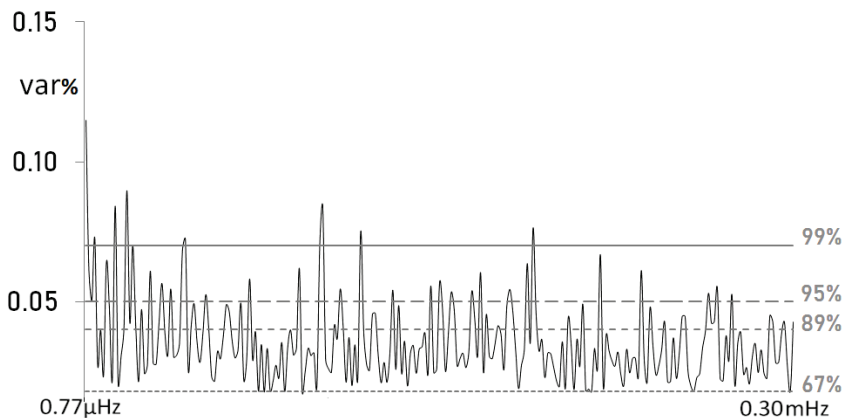


Figure 1. A preliminary spectrum of the moonquakes occurrences, computed for testing purposes in the Earth's natural band, 54'-15 days. While spectral magnitude response decreased an order of magnitude or more in absolute terms, a clear resemblance of the variance-spectrum of earthquakes occurrences from Omerbashich (2019a) strongly indicates that the superharmonic resonance drives the Moon seismotectonics too, and thus warrants further investigation. The spectral resolution used was $k = 1000$ points (lines). Corresponding spectral periods, matched to the orbital period-driven body resonance, are depicted per significance level on Figures 2 and 3 (stacked).

Statistical fidelity $\Phi > 12$ generally indicates a physically meaningful result for analyzing natural data sets (Omerbashich, 2006). Here, fidelity in the longest part of the 10 h–100 days band was increasing and at the longest detected period, of 89.3 days, has reached $\Phi = 1924.8 \gg 12$. On the other hand, fidelity became practically 0 (falling below the 10^{-1} labeled precision) shortly after the 50th subperiods of *theoretical sequences* (the series of resonance-forcing period's subperiods). Since $\Phi \in (\sim 1, \sim 12)$ characterized the most energetic resonance subband (as defined by the examined potential forcing-periods up to the 10 h high-ends), while taking on infinitesimal values (1, 0) for the most of the sequences beyond the 11th subperiods, that subband has defined the common strongest-energies subband as used in this paper.

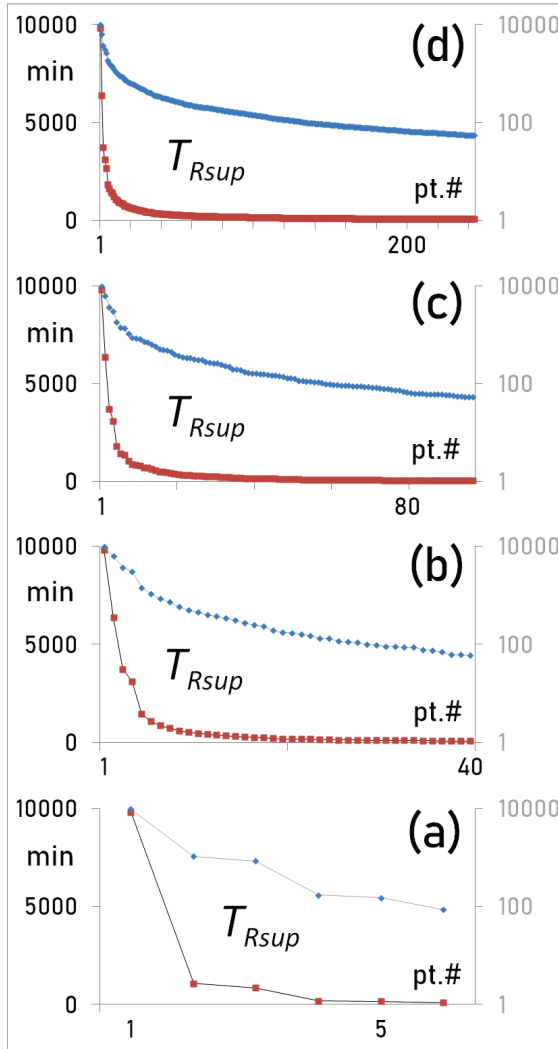


Figure 2. Significant periods in the preliminary spectra of 1969-1977 moonquakes' occurrences, Figure 1, per confidence level, in minutes: above 99% level (panel a), 95% (b), 89% (c), and 67% (d). The depiction's similarity with the earthquakes analysis of (Omerbashich, 2019a) prompted further investigation into the matching of the Moon's supposed theoretical superharmonic-resonance subperiods T_{Rsup} with respective nearest most significant spectral periods. The supposed T_{Rsup} in minutes (dark line) shown stacked against the same along the logarithmically scaled ordinate (light line), offset for legibility.

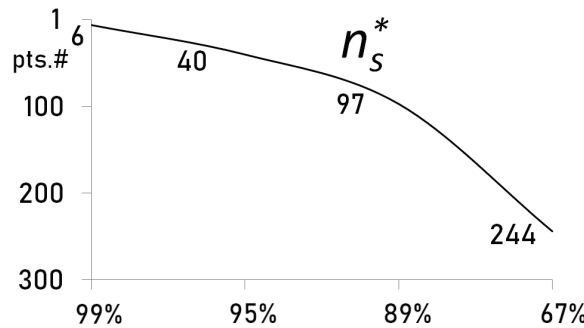


Figure 3. The overall number of statistically significant spectral points (lines) from the preliminary spectral analysis, Figure 1, per statistical significance level. The depiction's dissimilarity with (i.e., a steady change as seen here v. incoherent change as seen in) the same from earthquakes analysis by Omerbashich (2019a) indicates spectra of driven dynamics, i.e., a physical system in forced motion such that the system's vibration spectrum is insensitive to the choice of spectral resolution. The same for the Earth case had indicated a fully nonlinear physical system there – as due to rotating Earth's conjunctions in addition to the Moon-driven phase of the Earth. The stated dissimilarity then reflects a relative simplicity of the Moon case since the Moon, being spatially (tidally) locked to the overwhelming Earth, is not affected by the conjunctional component of non-linearity. That and the internal similarity of Figure 2 panels prompted further investigation into the matching of the Moon theoretical superharmonic-resonance subperiods with nearest respective spectral periods. For this, I double the spectral resolution and broaden the search for the solid Moon's driver phase to account for all lunar tides. Here additional periods are to be considered, so the band's boundaries were slid until the 10 h (27.78 μ Hz) cutoff was selected empirically as the Moon's natural band for demonstration and in order to stay on the safe side (owing to the mentioned lack of Moon reference models) when defining the separation between the strictly signal v. noise regions of the band of interest (practically: between the free- and forced-oscillation bands of the Moon).

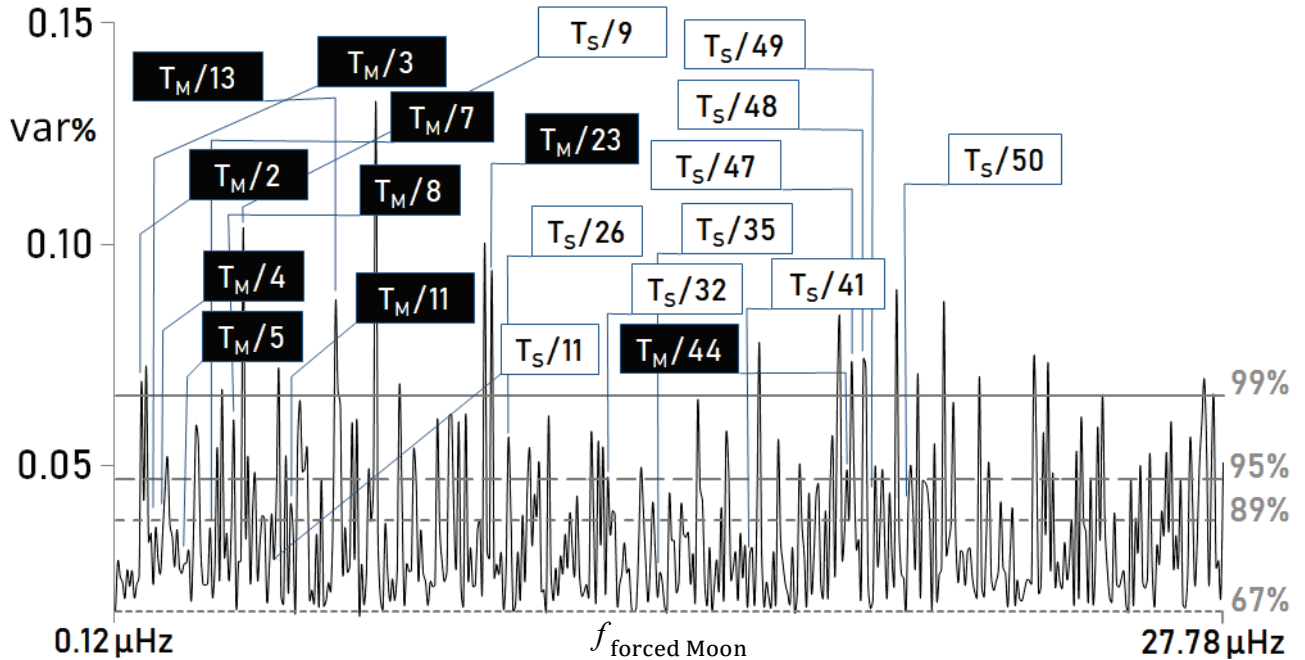


Figure 4. The spectrum of significant periods in all 12,474 occurrences of consecutive moonquakes from Day 208, 1969–Day 273, 1977. Spectral magnitudes are in percentage variance (var%), and resolution $k = 2000$ points (lines). Values corresponding to the depicted spectral peaks and theoretical superharmonic resonance subperiods are given in Tables 1 and 2. Labels are non-arbitrary, here attached to the cases of two physical lunar tides. Thus the highlighted labels mark the superharmonic resonance subperiods as driven by the Moon orbital (sidereal) period, and the transparent labels the noise signature of the superharmonic resonance subperiods as driven by the synodic period. The depiction is a visual pseudo-separation of the orbit-forced signal v. synodic-forced noise. The $27.78 \mu\text{Hz}$ cutoff was selected empirically, Figures 3 and 4, while the lower end was selected arbitrarily. That the used methodology and data treatment were justified is seen from the boost in all significant periods relative to the preliminary testing results of Figure 1. Note that the Moon orbital period, as used in this study, is not be confused with a selenocentric orbital period.

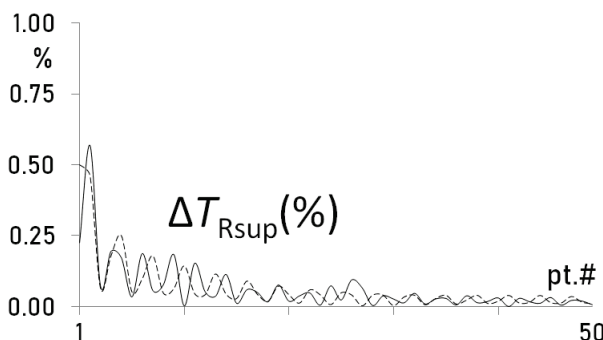


Figure 5. Relative match (Δ) of physical Moon-tidal periods' theoretical superharmonic resonance subperiods, with nearest respective periods from the computed spectra of moonquakes' occurrences, Figure 4, in % to the theoretical value. Shown are orbital period's matchings (solid line) v. synodic period's matchings (dashed line). The matchings stay well within 0.5 % and below 0.1 % most of the time.

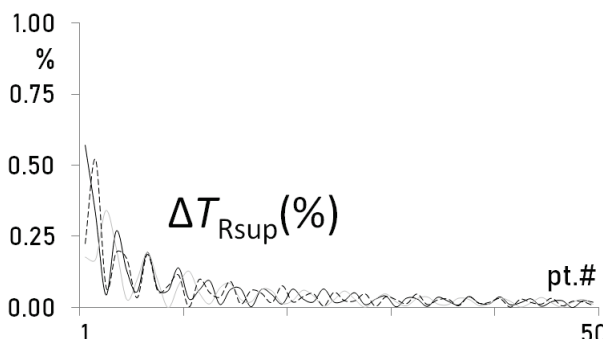


Figure 6. Relative match (Δ) of the astronomical tidal periods' theoretical superharmonic resonance subperiods, with nearest respective periods from the computed spectra of moonquakes' occurrences, Figure 4, in % to the theoretical value. Shown are anomalistic period's matchings (dark line) v. nodical period's matchings (dark dashed line) v. tropical period's matchings (light line). The matchings stay well within 0.5 % and below 0.1 % most of the time.

	39343.19040	42524.04960	ORBITAL'S	32	Φ	Δ [min]	[%]	SYNODIC'S	34	Φ	Δ [min]	[%]
1/2	19671.59520	21262.02480	19627.43761		44.8	44.15759	0.224	21368.56952	*		-106.54472	0.501
1/3	13114.39680	14174.68320	13039.90940		19.8	74.48740	0.568	14109.20498		23.2	65.47822	0.462
1/4	9835.79760	10631.01240	9842.91332		11.3	-7.11572	0.072	10624.34487	*		6.66753	0.063
1/5	7868.63808	8504.80992	7853.33115		7.2	15.30693	0.195	8519.97869	*		-15.16877	0.178
1/6	6557.19840	7087.34160	6568.45564	*		-11.25724	0.172	7069.67606	*		17.66554	0.249
1/7	5620.45577	6074.86423	5618.56616		3.7	1.88961	0.034	6071.75853	*		3.10570	0.051
1/8	4917.89880	5315.50620	4908.70025		2.8	9.19855	0.187	5320.71496	*		-5.20876	0.098
1/9	4371.46560	4724.89440	4373.91357	*		-2.44797	0.056	4716.47660		2.6	8.41780	0.178
1/10	3934.31904	4252.40496	3931.33118	*		2.98786	0.076	4250.42821	*		1.97675	0.046
1/11	3576.65367	3865.82269	3570.08558		1.5	6.56809	0.184	3868.20039		1.7	-2.37770	0.062
1/12	3278.59920	3543.67080	3278.54214	*		0.05706	0.002	3538.61851	*		5.05229	0.143
1/13	3026.39926	3271.08074	3031.02032		1.1	-4.62106	0.153	3269.64186		1.2	1.43888	0.044
1/14	2810.22789	3037.43211	2811.67036	*		-1.44247	0.051	3038.66738	*		-1.23527	0.041
1/15	2622.87936	2834.93664	2621.92589		0.8	0.95347	0.036	2838.17280		0.9	-3.23616	0.114
1/16	2458.94940	2657.75310	2456.17209	*		2.77731	0.113	2656.62551		0.8	1.12759	0.042
1/17	2314.30532	2501.41468	2314.56898	*		-0.26366	0.011	2502.09481	*		-0.68013	0.027
1/18	2185.73280	2362.44720	2184.43419	*		1.29861	0.059	2364.55339	*		-2.10619	0.089
1/19	2070.69423	2238.10787	2071.71131	*		-1.01708	0.049	2237.18223	*		0.92564	0.041
1/20	1967.15952	2126.20248	1966.83407	*		0.32545	0.017	2126.58003	*		-0.37755	0.018
1/21	1873.48526	2024.95474	1872.06368	*		1.42158	0.076	2026.39860	*		-1.44386	0.071
1/22	1788.32684	1932.91135	1788.65870	*		-0.33186	0.019	1932.12694	*		0.78441	0.041
1/23	1710.57350	1848.87172	1709.93745		0.3	0.63605	0.037	1849.07115	*		-0.19943	0.011
1/24	1639.29960	1771.83540	1640.08364	*		-0.78404	0.048	1772.86165		0.4	-1.02625	0.058
1/25	1573.72762	1700.96198	1573.65434	*		0.07328	0.005	1700.28175	*		0.68023	0.040
1/26	1513.19963	1635.54037	1514.29834	*		-1.09871	0.073	1635.62909		0.3	-0.08872	0.005
1/27	1457.15520	1574.96480	1457.49135	*		-0.33615	0.023	1575.71312	*		-0.74832	0.048
1/28	1405.11394	1518.71606	1406.43276		0.2	-1.31882	0.094	1518.11575	*		0.60031	0.040
1/29	1356.66174	1466.34654	1355.77127	*		0.89047	0.066	1466.36374		0.3	-0.01720	0.001
1/30	1311.43968	1417.46832	1311.48258	*		-0.04290	0.003	1418.02382	*		-0.55550	0.039
1/31	1269.13517	1371.74354	1268.65816		0.2	0.47701	0.038	1371.20646	*		0.53708	0.039
1/32	1229.47470	1328.87655	1229.79647	*		-0.32177	0.026	1328.84623		0.2	0.03032	0.002
1/33	1192.21789	1288.60756	1192.06384	*		0.15405	0.013	1289.02482	*		-0.41726	0.032
1/34	1157.15266	1250.70734	1157.68942	*		-0.53676	0.046	1250.22150	*		0.48584	0.039
1/35	1124.09115	1214.97285	1124.19158	*		-0.10043	0.009	1214.91036		0.2	0.06249	0.005
1/36	1092.86640	1181.22360	1092.57776		0.1	0.28864	0.026	1181.53907	*		-0.31547	0.027
1/37	1063.32947	1149.29864	1063.63183	*		-0.30236	0.028	1148.85516	*		0.44348	0.039
1/38	1035.34712	1119.05394	1035.28938	*		0.05774	0.006	1118.96941	*		0.08453	0.008
1/39	1008.79975	1090.36025	1008.41820	*		0.38155	0.038	1090.59911	*		-0.23886	0.022
1/40	983.57976	1063.10124	983.70941	*		-0.12965	0.013	1062.69336	*		0.40788	0.038
1/41	959.59001	1037.17194	959.41766		0.1	0.17235	0.018	1037.07226		0.1	0.09968	0.010
1/42	936.74263	1012.47737	937.02515		0.1	-0.28252	0.030	1012.65752	*		-0.18015	0.018
1/43	914.95792	988.93139	914.95847	*		-0.00055	0.000	988.55383	*		0.37756	0.038
1/44	894.16342	966.45567	893.90721		0.1	0.25621	0.029	966.34562	*		0.11005	0.011
1/45	874.29312	944.97888	874.43726	*		-0.14414	0.016	945.11332	*		-0.13444	0.014
1/46	855.28675	924.43586	855.18971	*		0.09704	0.011	924.08444	*		0.35142	0.038
1/47	837.08916	904.76701	837.35299		0.1	-0.26383	0.032	904.64996		0.1	0.11705	0.013
1/48	819.64980	885.91770	819.68688	*		-0.03708	0.005	886.01610		0.1	-0.09840	0.011
1/49	802.92225	867.83775	802.75080	*		0.17145	0.021	868.13439		0.1	-0.29664	0.034
1/50	786.86381	850.48099	787.01433		0.1	-0.15052	0.019	850.35937		0.1	0.12162	0.014
1/51	771.43511	833.80489	771.38860	*		0.04651	0.006	833.87456	*		-0.06967	0.008

99% 95% 89% 67% * below significance

Table 1

Omerbashich – Moon body resonance

	39678.55200	39185.59680	39343.07520	ANOMAL'S	37	Φ	Δ [min]	%	NODICAL'S	40	Φ	Δ [min]	%	TROPICAL'S	36	Φ	Δ [min]	%
1/2	19839.27600	19592.79840	19671.53760	19952.58890	*	-113.31290	0.571		19627.43761	44.8	-34.63921	0.177		19627.43761	44.8	44.09999	0.224	
1/3	13226.18400	13061.86560	13114.35840	13182.63418	*	43.54982	0.329		13039.90940	19.8	21.95620	0.168		13182.63418	*	-68.27578	0.521	
1/4	9919.63800	9796.39920	9835.76880	9924.01572	*	-4.37772	0.044		9763.12576	*	33.27344	0.340		9842.91332	11.3	-7.14452	0.073	
1/5	7935.71040	7837.11936	7868.61504	7957.09863	*	-21.38823	0.270		7853.33115	7.2	-16.21179	0.207		7853.33115	7.2	15.28389	0.194	
1/6	6613.09200	6530.93280	6557.17920	6604.47402	*	8.61798	0.130		6532.82800	*	-1.89520	0.029		6568.45564	*	-11.27644	0.172	
1/7	5668.36457	5597.94240	5620.43931	5671.48064	*	-3.11607	0.055		5592.47746	*	5.46494	0.098		5618.56616	3.7	1.87315	0.033	
1/8	4959.81900	4898.1960	4917.88440	4969.46051	*	-9.64151	0.194		4888.77567	*	9.42393	0.192		4908.70025	2.8	9.18415	0.187	
1/9	4408.72800	4353.95520	4371.45280	4405.91423	*	2.81377	0.064		4358.08693	*	-4.13173	0.095		4373.91357	*	-2.46077	0.056	
1/10	3967.85520	3918.55968	3934.30752	3970.20854	1.8	-2.35334	0.059		3918.54070	*	0.01898	0.000		3931.33118	*	2.97634	0.076	
1/11	3607.14109	3562.32698	3576.64320	3602.11730	*	5.02379	0.139		3559.53456	*	2.79242	0.078		3580.69933	*	-4.05613	0.113	
1/12	3306.54600	3265.46640	3278.58960	3305.53610	*	1.00990	0.031		3269.64186	1.2	-4.17546	0.128		3278.54214	*	0.04746	0.001	
1/13	3052.19631	3014.27668	3026.39040	3054.07785	*	-1.88154	0.062		3015.84109	1.1	-1.56441	0.052		3023.41165	*	2.97875	0.098	
1/14	2834.18229	2798.97120	2810.21966	2831.50046	*	2.68183	0.095		2798.60389	*	0.36731	0.013		2811.67036	*	-1.45070	0.052	
1/15	2645.23680	2612.37312	2622.87168	2644.95737	*	0.27943	0.011		2610.55992	*	1.81320	0.069		2621.92589	0.8	0.94579	0.036	
1/16	2479.90950	2449.09880	2458.94220	2481.47446	0.7	-1.56496	0.063		2451.17341	*	-2.07361	0.085		2461.19120	*	-2.24900	0.091	
1/17	2334.03247	2305.03511	2314.29854	2332.49872	*	1.53375	0.066		2305.70708	*	-0.67197	0.029		2314.56898	*	-0.27044	0.012	
1/18	2204.36400	2176.97760	2185.72640	2204.42484	*	-0.06084	0.003		2176.53908	0.6	0.43852	0.020		2184.43419	*	1.29221	0.059	
1/19	2088.34484	2062.39983	2070.68817	2089.68356	0.5	-1.33872	0.064		2061.07559	*	1.32424	0.064		2071.71131	*	-1.02314	0.049	
1/20	1983.92760	1959.27984	1967.15376	1983.02563	*	0.90197	0.045		1960.43124	0.4	-1.15140	0.059		1966.83407	*	0.31969	0.016	
1/21	1889.45486	1865.98080	1873.47977	1889.68686	*	-0.23200	0.012		1866.26211	*	-0.28131	0.015		1872.06368	*	1.41609	0.076	
1/22	1803.57055	1781.16349	1788.32160	1804.73981	0.4	-1.16926	0.065		1780.72514	*	0.43835	0.025		1788.65870	*	-0.33710	0.019	
1/23	1725.15443	1703.72160	1710.56849	1724.62839	*	0.52604	0.030		1702.68544	*	1.03616	0.061		1709.93745	0.34	0.63104	0.037	
1/24	1653.27300	1632.73320	1639.29480	1653.59406	*	-0.32106	0.019		1633.41088	*	-0.67768	0.042		1640.08364	*	-0.78884	0.048	
1/25	1587.14208	1567.42387	1573.72301	1588.17980	*	-1.03772	0.065		1567.51017	*	-0.08630	0.006		1573.65434	*	0.06867	0.004	
1/26	1526.09815	1507.13834	1513.19520	1525.80861	0.3	0.28954	0.019		1506.72082	*	0.41752	0.028		1512.39682	*	0.79838	0.053	
1/27	1469.57600	1451.31840	1457.15093	1469.94301	0.3	-0.36701	0.025		1450.47038	*	0.84802	0.058		1457.49135	*	-0.34042	0.023	
1/28	1417.09114	1399.48560	1405.10983	1416.35627	*	0.73487	0.052		1399.89398	0.2	-0.40838	0.029		1404.79235	*	0.31748	0.023	
1/29	1368.22593	1351.22748	1356.65777	1368.09137	0.2	0.13456	0.010		1351.20825	*	0.01923	0.001		1357.29913	*	-0.64136	0.047	
1/30	1322.61840	1306.18656	1311.43584	1323.00749	*	-0.38909	0.029		1305.79510	*	0.39146	0.030		1311.48258	*	-0.04674	0.004	
1/31	1279.95329	1264.05151	1269.13146	1279.43961	0.2	0.51368	0.040		1264.66182	*	-0.61031	0.048		1268.65816	0.2	0.47330	0.037	
1/32	1239.95475	1224.54990	1229.47110	1239.92488	*	0.02987	0.002		1224.79406	*	-0.24416	0.020		1229.79647	*	-0.32537	0.026	
1/33	1202.38036	1187.44233	1192.21440	1202.77780	0.2	-0.39744	0.033		1187.36311	*	0.07922	0.007		1192.06384	*	0.15056	0.013	
1/34	1167.01624	1152.51755	1157.14927	1166.66059	0.2	0.35565	0.030		1152.15216	*	0.36539	0.032		1157.68942	*	-0.54015	0.047	
1/35	1133.67291	1119.58848	1124.08786	1133.71537	*	-0.04246	0.004		1120.00996	0.1	-0.42148	0.038		1124.19158	*	-0.10372	0.009	
1/36	1102.18200	1088.48880	1092.86320	1102.57972	*	-0.39772	0.036		1088.62761	*	-0.13881	0.013		1092.57776	0.1	0.28544	0.026	
1/37	1072.39330	1059.07018	1063.32636	1072.15328	*	0.24002	0.022		1058.95597	*	0.11421	0.011		1063.63183	*	-0.30547	0.029	
1/38	1044.17242	1031.19992	1035.34408	1044.26564	*	-0.09322	0.009		1030.85887	*	0.34105	0.033		1035.28938	*	0.05470	0.005	
1/39	1017.39877	1004.75889	1008.79680	1017.79198	*	-0.39321	0.039		1005.05222	*	-0.29333	0.029		1008.41820	*	0.37860	0.038	
1/40	991.96380	979.63992	983.57688	991.81003	*	0.15377	0.016		979.70853	*	-0.06861	0.007		983.70941	*	-0.13253	0.013	
1/41	967.76956	955.74626	959.58720	967.89878	*	-0.12922	0.013		955.61155	*	0.13471	0.014		959.41766	0.1	0.16954	0.018	
1/42	944.72743	932.99040	936.73989	944.37227	0.1	0.35516	0.038		932.67150	0.1	0.31890	0.034		937.02515	0.1	-0.28526	0.030	
1/43	922.75702	911.29295	914.95524	922.66862	*	0.08840	0.010		911.49630	*	-0.20335	0.022		914.95847	*	-0.00323	0.000	
1/44	901.78527	890.58175	894.16080	901.94014	*	-0.15487	0.017		890.60223	*	-0.02048	0.002		893.90721	0.1	0.25359	0.028	
1/45	881.74560	870.79104	874.29056	881.47697	0.1	0.26863	0.030		870.64460	*	0.14644	0.017		874.43726	*	-0.14670	0.017	
1/46	862.57722	851.86080	855.28424	862.53899	*	0.03823	0.004		852.16434	*	-0.30354	0.036		855.18971	*	0.09453	0.011	
1/47	844.22451	833.73610	837.08671	844.39764	*	-0.17313	0.021		833.87456	*	-0.13846	0.017		837.35299	0.1	-0.26628	0.032	
1/48	826.63650	816.36660	819.64740	826.43622	*	0.20028	0.024		816.35339	*	0.01321	0.002		819.68688	*	-0.03948	0.005	
1/49	809.76637	799.70606	802.91990	809.76708	*	-0.00071	0.000		799.55336	*	0.15270	0.019		802.75080	*	0.16910	0.021	
1/50	793.57104	783.71194	786.86150	793.75707	*	-0.18603	0.023		783.94078	*	-0.22884	0.029		787.01433	0.1	-0.15283	0.019	
1/51	778.01082	768.34504	771.43285	777.86515	0.1	0.14567	0.019		768.43566	*	-0.09062	0.012		771.38860	*	0.04425	0.006	

Table 2

Table 1. Differential Spectral Analysis of the Apollo Moonquake Catalog – Moon's physical tides: the difference, Δ , or the match, in Earth minutes and % to the theoretical value, between theoretical resonance subperiods v. corresponding nearest computed periods from the spectra of moonquakes occurrences, Figure 4. Orbital period's matchings (dark background): 10 lead subperiods dominate motion in the strongest-energies subband defined by $\Phi \in (-1, \sim 12)$ fidelity, where seven subperiods are seen dominating the subband (driving the signal), while 40 final subperiods reveal the signal's noise imprint as defined by infinitesimal fidelity $0 \lesssim \Phi < 1$. Synodic period's matchings (light background): 10 lead subperiods reveal the period not driving the strong motion, and 40 final subperiods reveal the signal's noise imprint. Below-significance matchings, marked with a *, seen fitting the respective tidal period's resonant imprints in noise as every driver produces its sequence of resonant subperiods, but only the orbital period's sequence affects the solid Moon's vibration. By a match, I mean a spectral period nearby corresponding theoretical resonance subperiod, to within $\pm 0.5\%$ for the strongest-energies subband (the signal in the strict sense) and $\pm 0.1\%$ for noise. The criterion is based on the success of the Earth body resonance demonstration that had set the precision for the Moon case an order of magnitude lower from the declared precision in the Earth case, of $\pm 5\%$. This since the overall variance (data quality) dropped also an order of magnitude for the Moon relative to the Earth case, Figure 1. This meant that the Moon case had to be imposed higher stringency on than the Earth case - an order of magnitude or better.

Table 2. Differential Spectral Analysis of the Apollo Moonquake Catalog– Moon's astronomical tides: the difference, Δ , or the match, in Earth minutes and % to the theoretical value, between theoretical resonance subperiods v. corresponding nearest computed periods from the spectra of moonquakes occurrences, Figure 4. The first 10 subperiods are taken as possibly defining the strongest-energies part of the energy band as in Table 1, where the last 40 subperiods reveal the signal's imprint (if any) in noise as in Table 1. Matched were astronomical periods: anomalistic (dark gray background), nodical (gray background), and tropical (light gray background). All cases: the first 10 subperiods reveal that the respective period is not driving the strong motion, while the last 40 reveal the respective signal's imprint in noise. (Note that all 5 tropical period's matchings and all 3 nodical period's matchings in the strongest energies are in fact driven by the orbital period, Table 1, as the common source, making those 5+3 periods ghosts.) Below-significance matchings, marked with an *, are seen as always fitting the respective tidal period's resonant imprint in noise (i.e., each driver produces its own sequence of resonant subperiods, but neither sequence affects the solid Moon; see Table 1 for the antithesis demonstration). Color scheme is as in Table 1.

4. Discussion

I detected all of the fifty initial periods of a resonance subperiods-sequence as forced by the Moon's orbital phase, Table 1. Since the exact value of the Moon's natural period of vibration is unknown or highly uncertain at best, fifty is considered to be a sufficient sample size - according to the law of large numbers. Besides - from the physics point of view - it made sense to look only for the first 32 significant superharmonic resonance periods since already the 33rd was shorter more than twice the band's upper end and below significance (where most of the signal's noise imprint was).

The driving periods of solid-Moon resonance are the computed spectral periods that best match the corresponding theoretical subperiods in strongest resonance-energies (the longest-periodic part of the subband). Here I selected the first (longest) ten theoretical resonance periods as the cutoff for the strongest energies since the analyses have shown that statistical fidelity beyond the 11th resonance period drops by an order of magnitude, and by several resonance periods beyond the 51st drops to practically 0. Performance of each candidate-resonance-period is shown in Tables 3-5. As seen in Figures 5 and 6, astronomical periods matchings (Figure 6) had higher degrees of internal consistency than physical periods matchings (Figure 5). This is expected given the arbitrariness of the astronomical v. physical periods, as the latter represent the physics of the Moon more faithfully than the former ever could (except by sheer coincidence, as also shown herein).

As seen from the matching of theoretical resonance subperiods against the corresponding nearest spectral periods computed at $k = 2000$ point (lines) resolution, the tropical period's relatively better performance in (i.e., its 50%-match with) the strongest-energies portion of the band than any other astronomical period's, Table 3, is by chance. For if it was physically meaningful, then the other two arbitrary (astronomical) periods – anomalistic and nodical – would also perform in a like manner instead of failing. Besides, all five theoretical resonance periods in the longest part of the band that were matched by tropical period's resonance subperiods, Table 2, were also matched by the corresponding 5 of 7 orbital subperiods, Table 1, rendering all five strongest tropical subperiods as ghosts. The same can be seen for the nodical period also: all three of its matched resonance subperiods, Table 2, were also matched by the corresponding 3 of 7 of the orbital subperiods, rendering all three of the strongest nodical subperiods as ghosts too, Table 1. Finally, the number of overall matched periods (regardless of significance) in the tropical period's matching is still worse than in either the orbital or synodic period's cases, Table 3.

	T_O	T_S	T_T	T_A	T_N
Overall					
No. of significant:	<u>18</u>	16	14	13	10
No. of insignificant:	<u>32</u>	34	36	37	40
In strongest resonance energies					
No. of significant:	<u>7</u>	3	5	3	1
No. of insignificant:	<u>3</u>	7	5	7	9

Table 3. Performance of each of the Moon's long-periodic tidal periods of interest, in matching of their theoretical resonance subperiods with the corresponding nearest periods from the computed spectra of moonquakes occurrences, Figure 4 and Tables 1 and 2, according to the criterion of statistical significance (Yes/No) of the matched spectral period's peaks. The Moon's orbital period, T_O , as one of the two physical tides of the Moon (the other being the synodic, T_S) outperforms (underlined values) the synodic tide and all three astronomical tides (tropical, T_T ; anomalistic, T_A ; nodical, T_N) – both overall and in the strongest resonance energies subband, of 2.5–30 days ($\sim 0.4\text{--}4.6 \mu\text{Hz}$).

	T_O	T_S	T_T	T_A	T_N
$\sum \Delta (\%)$	3.13	3.26	2.83	3.05	2.64
No. of significant:	<u>18</u>	16	14	13	10
$\bar{\Delta}(\%)$	<u>0.17</u>	0.20	0.20	0.23	0.26

Table 4. Performance from Table 3, but according to the criterion of average matching in percents (the differences between theoretical resonance-subperiods and corresponding nearest computed spectral periods). As in Table 3, the Moon's orbital tide is again seen outperforming (underlined values) all other periods. The average was taken over the matched spectral periods statistically significant if at least 67% significant. This performance revealed that the matching of the orbital period's against the computed spectra of moonquakes not only outperforms other candidate forcers but is also physically meaningful. This performance has corroborated that considering both signal and its noise imprint together when extracting a physical process from natural data is valuable for low-quality records.

Importantly, due to a relatively small difference between the orbital and tropical periods, the orbital period excites not only the five strongest periods but 43 out of 50 of those in total. Finally, the orbital period outperforms other periods in the sense of average percentage-difference (percentage-matching) too, Table 4. Note also the astronomical periods' internal consistency outperforming the same of the physical (orbital and synodic) periods, Figures 6 v. 5. Since astronomical periods dominate the noise, this consistency translates into interference and thereby forbids that precession-driven resonance – such as that induced by the tropical period – spills over into the signal and becomes the driver of seismotectonics on the Moon (or the Earth as speculated in the past) as part of the Earth-Moon oscillator. The effect of astronomical periods on Moon's long-periodic information amounts to no more than ripples in selenophysical ambient noise.

As a key verification of the above result against known physics of the Moon, note that of the five Moon tides the anomalistic and nodical were found to be least involved in the generation of body resonance, Table 2. This is expected given their amplitudes of $\sim 0.1 \text{ m}$ that make them the two relatively largest vertical tides on the Moon (Seidelmann, 1992), thus hindering any secondary vibration including their own. Note also that the body resonance due to nonlinearity by an external phase disturbance is primarily a horizontal movement. Then in the absence of external forcing beyond the here examined lunar tides, the body resonance as computed herein is the likely culprit behind the Moon's “free” librations as well, which are thus made effectively unceasing.

The discovery of the overwhelming spectral response of the occurrences of moonquakes to the orbital phase's resonance subperiods verifies the well-known harmonically induced lunar seismotectonics. As with the Earth, the detected superharmonic resonance of the Moon $T_{R\text{sup}} = n / (mT)$ is of $n = T^2$ type, where $n / m \gg 1 \Rightarrow n \gg m$ characterizes the inducing process. In addition to revealing that seismotectonics universally is a resonance-induced process (even in a special case of tidally locked inferiors like the Moon to the Earth), this research indicates that the Moon's synchronization with its overwhelming Earth was, in fact, resonance-assisted (Thévenin et al., 2011). However, even as an indication, the find still validates the same definitive conclusion from the demonstration of the Earth body resonance.

5. Conclusions

Using spectra of moonquakes occurrences, I was able to verify that lunar seismotectonics arises in the harmonic response of Moon's inner regions ("tectonic plates"; bodies of mass) to the (range of at least 50 initial) resonance periods shown fully recoverable from the cataloged moonquakes occurrences. Thus tectonic (tidal) moonquakes are captured as "riding" on the resonance much like the tectonic earthquakes are. The T_M phase drives moonquakes and probably excites the so-called free librations of the Moon as well. No subharmonic resonance periods have been detected, which, given the fact that the Earth-locked Moon has only one external forcing phase, additionally supports the body resonance case for the Moon.

As with the Earth, the detection of the Moon's virtually entire resonance range means that its resonance is unceasing and that all of the Moon's inner regions respond actively to some of the resonance periods as those activate. Just as the Moon gives rise to the long-periodic resonance of the solid Earth, so does the Earth give rise to a long-periodic resonance of the solid Moon, confirming that the two bodies form a coupled mechanical oscillator in which the inferior body has attained the absolute synchronization, i.e., both spatially (orbital) and temporally (vibrational), while the superior body has attained a relative (temporal, i.e., vibrational) synchronization of 1 h (Omerbashich, 2019a). Thanks to the fact that the Moon is under a single external forcing, the moonquake prediction is considerably simpler to achieve than the earthquake prediction, pending quality lunar data.

Acknowledgments

I thank Dr. Ralph Lorenz (Johns Hopkins University) and Dr. Yosio Nakamura (University of Texas at Austin) for useful discussions and suggestions, Dr. Spiros Pagiatakis (York University) for providing his software LSSA v.5.0, and Barbara Pope (NASA/NSSDCA) for help with the data.

References

- Bulow, R.C., Johnson, C.L., Bills, B.G., Shearer, P.M.** (2007) Temporal and spatial properties of some deep moonquake clusters. *Journal of Geophysical Research* 112:E09003
- Den Hartog, J.** (1985). *Mechanical Vibrations* (4th Ed.) Dover Publications, New York
- Khan, A., Pommier, A., Neumann, G.A.** (2013) The lunar moho and the internal structure of the Moon: A geophysical perspective. *Tectonophysics* 609:331–352
- Nakamura, Y.** (2019) Professor Emeritus of Selenophysics, University of Texas at Austin. Personal Communication. 27-28 March
- Nakamura, Y., Latham, G.V., Dorman, H.J., Harris, J.E.** (1981) Passive Seismic Experiment, Long Period Event Catalog, Final Version (1969 Day 202 - 1977 Day 273, ALSEP Stations 11, 12, 13, 14, 15, and 16). Institute for Geophysics. Austin: University of Texas
- Omerbashich, M.** (2004) Earth-model discrimination method. ProQuest, Ann Arbor, Michigan, USA. pp.129
- Omerbashich, M.** (2006) Gauss-Vaníček Spectral Analysis of the Sepkoski Compendium: No New Life Cycles. *Computing in Science and Engineering* 8:26-30
- Omerbashich, M.** (2007) Magnification of mantle resonance as a cause of tectonics. *Geodinamica Acta* 20(6):369-383
- Omerbashich, M.** (2008) Stochastic resonance for exploration geophysics. arXiv:0810.5708
- Omerbashich, M.** (2019a) Earth body resonance. *Journal of Geophysics* 63(1):15-29
- Omerbashich, M.** (2019b) On solar origin of alleged mass-extinction periods in records of natural data. (**A.Y. Rozanov**, Ed.) *Paleontological Journal*. In press
- Pikovsky, A., Rosenblum, M., Kurths, J.** (2001) *Synchronization: A Universal Concept in Nonlinear Sciences* (Vol. 12). Cambridge, United Kingdom: Cambridge University Press
- Press, W.H., Teukolsky, S.A., Vetterling, W.T., Flannery, B.P.** (2007) *Numerical Recipes: The Art of Scientific Computing* (3rd Ed.). London, UK, Cambridge University Press
- Seidelmann, P.** (1992) *Explanatory Supplement to the Astronomical Almanac*. A revision to the Explanatory Supplement to the Astronomical Ephemeris and the American Ephemeris and Nautical Almanac. Mill Valley, CA, USA: University Science Books
- Thévenin, J., Romanelli, M., Vallet, M., Brunel, M., Erneux, T.** (2011) Resonance Assisted Synchronization of Coupled Oscillators: Frequency Locking without Phase Locking. *Physical Review Letters* 107:104101-1-5
- Vaníček, P.** (1969) Approximate Spectral Analysis by Least-Squares Fit. *Astrophysics and Space Science* 4(4):387–391
- Vaníček, P.** (1971) Further Development and Properties of the Spectral Analysis by Least-Squares Fit. *Astrophysics and Space Science* 12(1):10–33
- Yang, J.H., Sanjuán, M.A.F., Liu, H.G.** (2016) Vibrational subharmonic and superharmonic resonances. *Communications in Nonlinear Science and Numerical Simulation* 30(1-3):362–372.